HHS Public Access

Author manuscript

Transplantation. Author manuscript; available in PMC 2016 December 01.

Published in final edited form as:

Transplantation. 2015 December ; 99(12): 2494–2503. doi:10.1097/TP.0000000000000830.

Ex vivo Perfusion with Adenosine A2A Receptor Agonist Enhances Rehabilitation of Murine Donor Lungs after Circulatory Death

Mathew L. Stone, **Ashish K. Sharma**, **Valeria. R. Mas**, **Ricardo C. Gehrau**, **Daniel P. Mulloy**, **Yunge Zhao**, **Christine L. Lau**, **Irving L. Kron**, and **Victor E. Laubach**

Department of Surgery, University of Virginia, Charlottesville, VA

Mathew L. Stone: mstone@virginia.edu; Ashish K. Sharma: aks2n@virginia.edu; Valeria. R. Mas: vrm3n@virginia.edu; Ricardo C. Gehrau: rcg2d@virginia.edu; Daniel P. Mulloy: daniel.mulloy@gmail.com; Yunge Zhao: yz5u@virginia.edu; Christine L. Lau: cll2y@virginia.edu; Irving L. Kron: ilk@virginia.edu

Abstract

Background—*Ex vivo* lung perfusion (EVLP) enables assessment and rehabilitation of marginal donor lungs prior to transplantation. We previously demonstrated that adenosine A2A receptor ($A_{2A}R$) agonism attenuates lung ischemia-reperfusion injury. The current study utilizes a novel murine EVLP model to test the hypothesis that $A_{2A}R$ agonist enhances EVLP-mediated rehabilitation of donation after circulatory death (DCD) lungs.

Methods—Mice underwent euthanasia and 60 min warm ischemia, and lungs were flushed with Perfadex and underwent cold static preservation (CSP, 60 min). Three groups were studied: no EVLP (CSP), EVLP with Steen solution for 60 min (EVLP), and EVLP with Steen solution supplemented with ATL1223, a selective $A_{2A}R$ agonist (EVLP+ATL1223). Lung function, wet/dry weight, cytokines and neutrophil numbers were measured. Microarrays were performed using the Affymetrix GeneChip Mouse Genome 430A 2.0 Array.

Results—EVLP significantly improved lung function versus CSP, which was further, significantly improved by EVLP+ATL1223. Lung edema, cytokines and neutrophil counts were reduced after EVLP and further, significantly reduced after EVLP+ATL1223. Gene array analysis revealed differential expression of 1,594 genes after EVLP, which comprise canonical pathways involved in inflammation and innate immunity including IL-1, IL-8, IL-6 and IL-17 signaling. Several pathways were uniquely regulated by EVLP+ATL1223 including the downregulation of genes involved in IL-1 signaling such as ADCY9, ECSIT, IRAK1, MAPK12 and TOLLIP.

Conclusion—EVLP modulates pro-inflammatory genes and reduces pulmonary dysfunction, edema and inflammation in DCD lungs, which are further reduced by $A_{2A}R$ agonism. This murine EVLP model provides a novel platform to study rehabilitative mechanisms of DCD lungs.

Corresponding author: Victor E. Laubach, PhD, Department of Surgery, University of Virginia, P.O. Box 801359, Charlottesville, VA 22908, laubach@virginia.edu.

Disclosure: The authors declare no conflicts of interest.

Authorship: LS, AKS, VRM, CLL, ILK and VEL contributed to research design. MLS, AKS, VRM, RCG, DPM and YZ contributed in the performance of the research. MLS, VRM and RCG participated in data analysis. MLS, VRM and VEL participated in manuscript writing.

Keywords

Lung transplantation; donation after circulatory death; ex situ lung perfusion; ischemia-reperfusion injury; cytokines; gene array

Introduction

Lung transplantation provides the only curative option for many patients with end-stage pulmonary disease, yet the success of lung transplantation is significantly limited by a shortage in donor organs and the inherent threat of ischemia-reperfusion (IR) injury that leads to primary graft dysfunction (PGD). Advancements over the past decade have decreased incidences of PGD from 30% to 5-15% while also expanding the number of donor lungs suitable for transplantation (1-7). Currently a significant donor organ shortage exists for lung transplantation, which contributes to a waiting list mortality that has increased to 15.7 per 100 wait-list years (7). A principle initiative in lung transplantation research is the utilization of DCD (donation after circulatory death, previously referred to as donation after cardiac death or non-heartbeating organ donation) lungs, which currently account for <2% of lung transplants performed within the United States (7). Traditionally associated with higher rates of IR injury, mortality, and long-term graft failure, DCD lungs introduce the need for reproducible and effective standards for organ assessment and rehabilitation to support clinical adoption and to meet the need for an increasing number of individuals awaiting lung transplantation (8, 9).

Ex vivo lung perfusion (EVLP, also known as ex situ lung perfusion) is a technique that provides normothermic perfusion and mechanical ventilation to donor lungs, allowing functional assessment during the preservation period (10). EVLP has been utilized as an effective strategy for the assessment of marginal, high-risk donor lungs and has also demonstrated potential for expansion of the limited donor organ pool through the rehabilitation of DCD lungs (11-14). While current advancements in EVLP-mediated rehabilitation merit optimism concerning the future utilization of DCD lungs, two principle benefits to this approach that have not been adequately explored are the delivery of therapeutic, anti-inflammatory agents to the injured lung and the identification of molecular markers that may serve as predictors of PGD after transplantation.

We have previously demonstrated that adenosine A2A receptor ($A_{2A}R$) agonism is a well-defined approach for the amelioration of lung IR injury after transplant (4, 15-17) largely through activation of $A_{2A}Rs$ on immune cells such as neutrophils and iNKT cells (5, 18). We have also shown that EVLP-mediated delivery of $A_{2A}R$ agonist is a potentially effective strategy for the rehabilitation of Maastricht category I DCD lungs (12). Thus, the purpose of the current study was twofold: 1) to establish and utilize a novel murine EVLP model to test the hypothesis that administration of a selective $A_{2A}R$ agonist during EVLP provides a superior strategy to EVLP alone for the rehabilitation of DCD lungs and 2) to assess changes in the gene expression profile in DCD lungs after EVLP.

Materials and Methods

Detailed methods are presented in the supplemental digital content (see SDC, Materials and Methods).

Animals

This study used 9-12 week old male C57BL/6 mice (Jackson Laboratory, Bar Harbor, ME). This study conformed to the National Institutes of Health guidelines and was conducted under animal protocols approved by the University of Virginia's Institutional Animal Care and Use Committee.

Murine Lung DCD Procedure

Mice were anesthetized and euthanized by cervical dislocation followed by a 60-minute period of “no-touch” warm ischemia. The left atrium was then vented via an atriotomy followed by infusion of the lungs with 3 mL 4°C Perfadex® solution (Vitrolife Inc., Denver, CO) supplemented with THAM Solution (Vitrolife, Kungsbacka, Sweden). The chest was then packed with ice and the lungs underwent cold static preservation (CSP) for 60 minutes at 4°C. Mice were then randomized into three groups: 1) CSP alone with no EVLP, 2) EVLP with Steen solution and 3) EVLP with Steen solution supplemented with the highly selective $A_{2A}R$ agonist, ATL1223 (30 nM, Lewis and Clark Pharmaceuticals, Charlottesville, VA). ATL1223 was chosen as the $A_{2A}R$ agonist because we have previously demonstrated that ATL1223 potently attenuates IR injury in mouse models and in a porcine lung transplantation model and because ATL1223 is a more potent and selective $A_{2A}R$ agonist versus earlier generation agonists (unpublished studies). Mice treated with ATL1223 during EVLP also received ATL1223 during the Perfadex flush (30 nM) prior to CSP whereas the EVLP group received vehicle (DMSO) during the flush. CSP lungs, which did not undergo EVLP with Steen solution, underwent immediate functional assessment after re-intubation as described below in order to define the status of the lungs at the initiation of EVLP.

Murine EVLP

A diagram of the murine EVLP system is shown in Figure 1. Lungs were ventilated in the chest with room air following a tracheostomy. Following a right ventriculotomy, the pulmonary artery was cannulated for placement onto a murine isolated, lung perfusion apparatus (Hugo Sachs Elektronik, March-Huggstetten, Germany) as previously described (19). The left atrium was cannulated for drainage of the perfusate. The lungs were perfused with Steen solution (EXVIVO Perfusion Inc., Englewood CO) at a constant rate of 60 μl/g body weight/minute (20, 21). Steen solution within the circuit was gradually warmed from 4°C to 37°C (over approximately 10 minutes), and EVLP continued for 60 minutes. Steen solution was supplemented with 10,000 IU heparin, 500 mg cefazolin and 500 mg methylprednisolone per 1500 mL, modeling preclinical and clinical EVLP protocols (10, 12). Steen solution was also supplemented with vehicle (DMSO) for the EVLP group or ATL1223 (30 nM) for the ATL1223-treated group.

Lung Function

Pulmonary function and hemodynamic measurements were recorded throughout EVLP using the PULMODYN data acquisition system (Hugo Sachs Elektronik) as previously described (21). To measure lung function of the CSP group, lungs were placed directly on the isolated lung perfusion apparatus and perfused with standard Krebs-Henseleit buffer for a 5-minute equilibration period before data was recorded for an additional 5 minutes. These CSP lungs were utilized to obtain the data shown in Figures 2-6. A separate group of CSP lungs were perfused with Krebs-Henseleit buffer for one hour and compared to the EVLP and EVLP+ATL1223 groups in order to assess temporal changes in function during perfusion (see SDC Figure 1).

Cytokine Measurements

Using separate groups of animals, proinflammatory cytokines were measured in whole lung lysates using a multiplex cytokine panel assay (Bio-Rad Laboratories, Hercules, CA) as described previously (5, 21).

Neutrophil Counts

Using separate groups of animals, calculation of neutrophil numbers per high-powered field were performed on immunostained lung sections as described previously (21).

Lung Wet/Dry Weight

Right lungs were weighed and desiccated until a stable dry weight was achieved to calculate the lung wet/dry weight as an indicator of edema.

Statistical Analysis

Statistical analyses were performed using GraphPad Prism 6.0 software, and data are presented as the mean ± standard error of the mean. One-way ANOVA with post-hoc Tukey's multiple comparison test was performed to compare experimental groups. Statistical significance was set at $P < 0.05$.

RNA Isolation and Microarray Hybridization

Using separate groups of animals, total RNA was extracted from whole lungs using TRIzol reagent (Life technologies, Carlsbad, CA), following the Affymetrix GeneChip® Expression Analysis Manual (Affymetrix, Santa Clara, CA, USA) guidelines and recommendations. All RNA samples met purity and integrity quality control criteria previously established (22, 23). Reactions for cDNA synthesis and *in vitro* transcription for labeled cRNA probe, microarray hybridization, image generation, and probesets reading process were performed as reported previously (22). In total, twelve Affymetrix GeneChip Mouse Genome 430A 2.0 microarrays were hybridized for three separate groups of animals (n=4/group). After hybridization, each chip was scanned on an Affymetrix GeneChip® Scanner 3000 G7. Raw intensities for every probe were stored in electronic files (.DAT and .CEL formats) by the GeneChip® Operating Software (GCOS).

Microarray Quality Control and Data Analysis

The hybridized Affymetrix GeneChip Mouse Genome 430A 2.0 microarrays were analyzed using RMAexpress software to normalize probeset data by quantile normalization and summarized with median polish summarization using the Robust Multiarray Average method (24, 25). Pairwise comparisons (EVLP *vs.* CSP and EVLP+ATL1223 *vs.* CSP) were fit using two-sample *t*-test in the R programming environment (26). To adjust for the multiple hypothesis tests, the *p*-values were used in estimating the false discovery rate (FDR) using the Benjamini and Hochberg method (27-29). *P*-values ≤ 0.001 under a controlled FDR < 1% were considered significant. Fold-change values were used for differential expression magnitudes.

Interaction Networks, Functional Analysis and Upstream regulators

The Ingenuity Pathway Analysis (IPA, www.ingenuity.com) tool was used to analyze gene ontology and pathways of differential expressed genes. *P*-values ≤0.05 were considered significant. Spreadsheet lists containing probesets ID and fold-changes were generated and uploaded to IPA.

Results

ATL1223 Improves Lung Function and Reduces Edema During EVLP of DCD Lungs

DCD lungs undergoing EVLP demonstrated significantly increased pulmonary compliance (3.70±0.13 vs. 1.88±0.21 μl/cm H_2O, respectively) and decreased pulmonary artery pressure (9.22±0.21 vs. 14.14±0.37 cm H_2O, respectively) after 1 hour of perfusion compared to CSP lungs (Figure 2). In addition, EVLP significantly reduced pulmonary edema as assessed by wet/dry weight compared to CSP lungs (4.58±0.13 vs. 5.15±0.18, respectively) (Figure 2). Furthermore, EVLP with Steen solution supplemented with ATL1223 significantly increased pulmonary compliance (5.17±0.15 vs. 3.70±0.13 μl/cm H_2O, respectively) and reduced pulmonary artery pressure (7.79±0.22 vs. 9.22±0.21 cm H_2O, respectively) when compared to EVLP alone after 1 hour of perfusion (Figure 2). Temporal measurements of lung function during the 1 hour perfusion period demonstrate that function in the EVLP + ATL1223 group began to significantly diverge from the EVLP group by 30 minutes of perfusion and that lung function in the CSP group did not significantly change when perfusion was extended to one hour (SDC, Figure 1). In accordance with functional improvement, EVLP with ATL1223 also significantly reduced pulmonary edema compared to EVLP alone (4.08±0.10 vs. 4.58±0.13, respectively).

EVLP with ATL1223 Reduces Pro-Inflammatory Cytokine Expression

Expression of CXCL1, CCL2 and TNF-α were reduced in lungs following EVLP, although this did not reach significance (Figure 3). Treatment with ATL1223 during EVLP significantly reduced the levels of CXCL1, CCL2 and TNF-α versus EVLP alone. CXCL1 results for CSP, EVLP and EVLP+ATL1223 groups were: 78.9±37.6, 19.6±4.4 and 4.8±0.4 pg/ml, respectively. CCL2 results for CSP, EVLP and EVLP+ATL1223 groups were: 319.7±78.7, 208.4±46.2 and 89.8±20.2 pg/ml, respectively. TNF-α results for CSP, EVLP

and EVLP+ATL1223 groups were: 268.4±24.6, 210.0±39.5 and 150.4±19.0 pg/ml, respectively.

EVLP with ATL1223 Reduces Lung Neutrophil Numbers

Immunostaining of lung sections revealed a small decrease in neutrophil numbers after EVLP versus CSP, although this was not significant (Figure 4). However, EVLP with ATL1223 significantly reduced neutrophil numbers versus both CSP and EVLP groups (2.06±0.34 vs. 5.42±1.13 and 4.06±0.77, respectively).

Gene Expression Profiles in DCD Lungs After EVLP

EVLP of DCD lungs resulted in the differential expression of 1,594 genes (1,762 probesets) compared to CSP (Figure 5A). Core analysis was performed to interpret the data set in the context of biological processes, canonical pathways and molecular networks. The top two networks identified from the dataset included 1) connective tissue development and function, tissue morphology, cell cycle (score 36, score ≥5 was considered significant) and 2) molecular transport, skeletal and muscular system development and function, free radical scavenging (score 31).

From the analysis of molecular and cellular functions using the differentially expressed genes between the EVLP *vs.* CSP groups, cell death and survival (*p*-value range=1.15E-09–1.06E-02, 299 genes), gene expression (*p*-value range=1.39E-08–8.38E-04, 179 genes) and lipid metabolism (*p*-value range=4.59E-08–1.07E-02, 153 genes) were identified as the more relevant between the groups. A total of 123 canonical pathways were identified as significant and associated with the EVLP gene expression profile when compared to CSP ($p<0.05$; see SDC Table 1). From these canonical pathways, ten selected pathways focusing on inflammation and innate immune responses are highlighted in Figure 6A including IL-1 signaling (*p*-value=3.5E-04), IL-8 signaling (*p*-value=5.0E-04) and IL-17 signaling (*p*-value=1.7E-02). Further analysis of the IL-1 and IL-8 signaling pathways showed an important number of genes down-regulated by EVLP including IL6ST, SOCS3, PIK3CA, PIK3C2A, PIK3R1, MAPK13, TRAF6, FOS, JUN, CRP, PIK3CD, TNFRSF1B, IL1RAP, TNF and ATM, among others. Overall, as shown in Figure 6A, these pathways showed a higher percentage of genes down-regulated in the EVLP group.

Differential Gene Expression Analysis in DCD Lungs After EVLP+ATL1223

A comparison between the EVLP+ATL1223 and CSP groups resulted in a total of 1,917 differentially expressed genes, with 1,116 genes overlapping with the EVLP *vs.* CSP comparison analysis (Figure 5A). This indicates an important overlap between affected biological pathways in both EVLP conditions. However, the number of unique genes affected in the EVLP+ATL1223 *vs.* CSP analysis was higher than in the EVLP *vs.* CSP analysis. A direct comparison analysis of EVLP *vs.* EVLP+ATL1223 revealed a limited number of genes differentially expressed between these groups even when a flexible cutoff for significance (p-value<0.001) was used (Figure 5B).

When comparing EVLP+ATL1223 to CSP, the top molecular and cellular functions associated with the statistical differentially expressed genes included 1) gene expression (*p*-

value range=3.7E-22–3.2E-04, 427 genes), 2) cellular growth and proliferation (*p*-value range=3.3E-20–3.1E-04, 627 genes) and 3) cell death and survival (*p*-value range=1.1E-16–3.7E-04, 596 genes). A total of 166 canonical pathways were identified as significant and associated with the EVLP+ATL1223 gene expression profile when compared to CSP ($p<0.05$; see SDC Table 2). From these canonical pathways, ten selected pathways focusing on inflammation and innate immune responses are highlighted in Figure 6B including IL-1 signaling (*p*-value=3.0E-03), IL-8 signaling (*p*-value=2.7E-02) and IL-17 signaling (*p*-value=3.6E-02). Interestingly, the evaluation of unique genes differentially expressed in EVLP+ATL1223 *vs.* CSP showed an overall effect of down-regulation of genes related to NF-κB signaling, among other pathways (9 in total), with most of these genes down-regulated in EVLP+ATL1223*vs*. CSP (Figure 6C).

Identification of Differential Gene Expression Profiles Associated with EVLP+ATL1223 versus EVLP Alone

To evaluate differences strictly associated with ATL1223 treatment during EVLP, we compared EVLP and EVLP+ATL1223 to the same CSP group and performed comparison analysis using IPA. From the analysis, a noticeably greater number of IL-1 signaling genes were down-regulated in the EVLP+ATL1223 group including down-regulation of ADCY9, ECSIT, IRAK1, MAPK12 and TOLLIP (Table 1); indicating a greater effect in the number of inflammatory genes decreased with the use of ATL1223. Also, a similar effect was observed for acute phase response signaling with an additional number of genes down-regulated in the EVLP+ATL1223 group including PTPN11, MAP3K5, CP, PDPK1, SOCS5, MAPK12, TRADD, MAP3K7 and IRAK1 (data not shown).

Discussion

Our group and others have demonstrated in preclinical models that DCD lungs with extended warm ischemic times (up to 60 minutes) may be rehabilitated by EVLP to an acceptable state for transplantation (12, 13). These results have been furthered by clinical studies in which initially-rejected human donor lungs have been rehabilitated to acceptable standards for transplantation (30, 31). While these results support a promising future for use of DCD lungs in successful transplantation, not all lung grafts are recoverable and many experience a decrease in oxygenation capacity with an increase in interstitial edema during EVLP (32). The future application of EVLP is, therefore, dependent on early, targeted therapy and the establishment of predictive standards for post-transplantation lung function. For example, experimental studies have identified nebulized arginase inhibitor and adenoviral vector delivery of IL-10 as potential rehabilitative strategies during EVLP (33, 34). Furthermore, an understanding of the mechanisms that underlie EVLP-mediated rehabilitation would lead to the advancement of this technique for lung transplantation.

The present study introduces a novel murine model of EVLP of DCD lungs, which provides a fundamental framework for future studies aimed toward identifying potential predictive markers of PGD after EVLP and transplantation as well as the assessment of novel targeted therapies for EVLP-mediated donor lung rehabilitation. Importantly, our study demonstrates that EVLP of DCD lungs leads to significantly improved function and reduced edema.

$A_{2A}R$ agonism has been established as an effective strategy for the prevention of IR injury after experimental lung transplantation (4, 12, 15-17). Recently, using a porcine model, our group has demonstrated that $A_{2A}R$ agonist therapy provides effective EVLP-mediated rehabilitation of heart-beating donor lungs after extended cold ischemic preservation (35). While this study demonstrated the potential for translation of this therapy to clinical transplantation, no comparative analysis of EVLP-mediated $A_{2A}R$ agonist treatment has been previously performed in DCD lungs. Thus, the present study utilizes the murine EVLP model to demonstrate enhanced rehabilitation of DCD lungs via $A_{2A}R$ agonist therapy, which results in significantly improved lung function as well as reduced edema and inflammation.

Although EVLP improved function of murine DCD lungs, EVLP resulted in small reductions of pro-inflammatory cytokine levels and neutrophil counts that were not statistically significant. It is possible that EVLP with Steen solution largely preserves endothelial function to attenuate edema and dysfunction, resulting in more indirect effects on cytokine expression during reperfusion. Importantly, EVLP with $A_{2A}R$ agonist treatment significantly decreased pro-inflammatory cytokine levels and neutrophil numbers, two established hallmarks of lung IR injury and PGD (36).

Because lungs are perfused with acellular Steen solution, neutrophil numbers in lungs were overall lower than what is typically observed after IR *in vivo* (21). As shown in figure 4, it is likely that most observed neutrophils are marginated (i.e. temporarily adhered to endothelium). We have previously shown that buffer perfusion of isolated murine lungs does not readily wash away significant numbers of marginated neutrophils (20). Although EVLP may have slightly decreased the number of marginated neutrophils, the inclusion of ATL1223 with EVLP resulted in significantly fewer neutrophils. This suggests that $A_{2A}R$ agonism reduces the adhesion of marginated neutrophils, which is supported by studies showing that $A_{2A}R$ agonists modulate adhesion molecule expression (37) and inhibit neutrophil transuroepithelial migration (38). Because neutrophil activation and infiltration is a key component of IR injury, the flushing away of greater numbers of marginated neutrophils in DCD lungs by EVLP-mediated $A_{2A}R$ agonist delivery would be beneficial in attenuating IR injury after transplantation.

A traditional measure of lung function during EVLP, often used to predict successful transplantation, has been the partial pressure of oxygen (PO_2) in the EVLP perfusate. However, this may be misleading since Yeung *et al*. used a preclinical study of high-risk donor lungs to demonstrate a higher predictive value for decreased compliance and increased airway pressure than PO_2 during EVLP (39). Thus Yeung *et al*. demonstrated that one cannot place the full emphasis of lung assessment on PO_2 during EVLP and that *ex vivo* PO_2 may not be the first indication of lung injury (39). Although PO_2 levels during EVLP were not measured in the present study, our results support the concept that pulmonary compliance and pulmonary artery pressure may be useful and important physiologic predictors of graft function.

Gene expression analysis revealed a large number of canonical pathways, including many associated with inflammation and innate immune responses, that are significantly affected

by EVLP, with the overall affect being downregulation of most genes in these pathways. The induction of inflammatory responses after reperfusion is believed to be the major contributor to IR injury and PGD after transplantation, and the present study suggests that proinflammatory responses in DCD lungs occur quickly after perfusion and that EVLP with Steen solution effectively attenuates these responses via modulation of the expression of many proinflammatory genes. Although treatment with ATL1223 during EVLP resulted in a limited number of differentially expressed genes compared to EVLP without ATL1223, a larger number of canonical pathways overall were significantly affected after EVLP with ATL1223. Gene analysis demonstrated the modulation of multiple and overlapping inflammatory pathways after EVLP with or without ATL1223. It is possible that some of these may be useful biomarkers to assess inflammation in lungs during EVLP as a potential means to gauge the acceptability of DCD lungs for successful transplantation.

There are several limitations to the current study. First, the circuit design is ‘open’ rather than ‘closed’ as typically utilized in clinical EVLP protocols. This may actually introduce the potential for improved efficacy, as the murine model drains perfusate through the left atrium and may more effectively clear both pro-inflammatory cytokines and neutrophils that would persist in a closed circuit. While recognizing this limitation, many advocate a standardized approach of Steen solution replacement during EVLP (10), and the present study supports the potential benefit of this approach. Second, murine lungs were assessed *ex vivo* but were not transplanted. While murine models of transplantation exist, the focus of this initial study was to evaluate lung function and injury during EVLP, and thus these results could not be translated to transplanted lungs. Third, EVLP was performed for 1 hour where as clinical EVLP is typically performed for 4 hours (or even longer). Although 1 hour of EVLP was sufficient for significant improvements in lung function and edema, it is possible that a longer period of EVLP would lead to more significant effects on inflammation markers such as cytokines or gene expression. Preliminary studies indicated that perfused lungs typically stabilize within 30 minutes and remain stable throughout 1 hour of perfusion and beyond, thus we chose to assess lungs after 1 hour. Fourth, it is possible that anti-inflammatory effects of methylprednisolone could have an influence on lung inflammation (e.g. cytokine levels) during EVLP. Steen solution was supplemented with methylprednisolone (as well as heparin and cefazolin) in order to model what is used in many preclinical and clinical EVLP protocols. However, both the EVLP and EVLP +ATL1223 groups of lungs were perfused with identical perfusate (+/- ATL1223) and thus were directly comparable. Finally, it is possible that the beneficial effects of ATL1223 during EVLP could be due to the vasodilatory actions of $A_{2A}R$ agonism as shown by many studies. However, this is unlikely since the dose of $A_{2A}R$ agonist required for cardiovascular effects are much higher than the dose required for inhibition of inflammation, and the dose of ATL1223 utilized in the present study was based on well-established doses used in prior studies that prevent IR injury but do not have significant cardiovascular effects (15, 16, 40).

In conclusion, the present study demonstrates that EVLP provides an effective platform for the rehabilitation of DCD lungs in a novel murine model. EVLP-mediated therapy with $A_{2A}R$ agonist results in significantly enhanced protection as demonstrated by reductions inpulmonary dysfunction, edema, pro-inflammatory cytokines and neutrophil numbers.

Additionally, a decrease in the expression of genes associated with inflammation was observed after EVLP. The murine EVLP model provides a reproducible and effective means for experimental, mechanistic studies of novel EVLP-directed therapies that may help in the identification of predictive biomarkers of lung function after EVLP and transplantation. Future translation of EVLP and $A_{2A}R$ agonist therapy to DCD lungs could greatly impact all lung transplant recipients by not only increasing the donor pool size to reduce the wait-list mortality but may also attenuate PGD leading to improved short- and long-term outcomes for lung transplant patients.

Supplementary Material

Refer to Web version on PubMed Central for supplementary material.

Acknowledgments

Funding: This work was supported by NIH R01HL077301 (V.E.L.), NIH R01HL119218 (V.E.L. and I.L.K.) and NIH T32HL007849 (I.L.K.).

References

1. Cypel M, Rubacha M, Yeung J, et al. Normothermic ex vivo perfusion prevents lung injury compared to extended cold preservation for transplantation. Am J Transplant. 2009; 9:2262. [PubMed: 19663886]
2. de Perrot M, Liu M, Waddell TK, Keshavjee S. Ischemia-reperfusion-induced lung injury. Am J Respir Crit Care Med. 2003; 167:490. [PubMed: 12588712]
3. Sanchez PG, Bittle GJ, Williams K, et al. Ex vivo lung evaluation of prearrest heparinization in donation after cardiac death. Ann Surg. 2013; 257:534. [PubMed: 23108122]
4. Gazoni LM, Walters DM, Unger EB, Linden J, Kron IL, Laubach VE. Activation of A1, A2A, or A3 adenosine receptors attenuates lung ischemia-reperfusion injury. J Thorac Cardiovasc Surg. 2010; 140:440. [PubMed: 20398911]
5. Sharma AK, Laubach VE, Ramos SI, et al. Adenosine A2A receptor activation on CD4+ T lymphocytes and neutrophils attenuates lung ischemia-reperfusion injury. J Thorac Cardiovasc Surg. 2010; 139:474. [PubMed: 19909990]
6. Cypel M, Yeung JC, Liu M, et al. Normothermic ex vivo lung perfusion in clinical lung transplantation. N Engl J Med. 2011; 364:1431. [PubMed: 21488765]
7. Valapour M, Paulson K, Smith JM, et al. OPTN/SRTR 2011 Annual Data Report: lung. Am J Transplant. 2013; 13(Suppl 1):149. [PubMed: 23237700]
8. de Antonio DG, Marcos R, Laporta R, et al. Results of clinical lung transplant from uncontrolled non-heart-beating donors. J Heart Lung Transplant. 2007; 26:529. [PubMed: 17449425]
9. de Antonio DG, de Ugarte AV. Present state of nonheart-beating lung donation. Curr Opin Organ Transplant. 2008; 13:659. [PubMed: 19060559]
10. Cypel M, Yeung JC, Hirayama S, et al. Technique for prolonged normothermic ex vivo lung perfusion. J Heart Lung Transplant. 2008; 27:1319. [PubMed: 19059112]
11. Dong B, Stewart PW, Egan TM. Postmortem and ex vivo carbon monoxide ventilation reduces injury in rat lungs transplanted from non-heart-beating donors. J Thorac Cardiovasc Surg. 2013; 146:429. [PubMed: 23260460]
12. Mulloy DP, Stone ML, Crosby IK, et al. Ex vivo rehabilitation of non-heart-beating donor lungs in preclinical porcine model: delayed perfusion results in superior lung function. J Thorac Cardiovasc Surg. 2012; 144:1208. [PubMed: 22944084]
13. Nakajima D, Chen F, Yamada T, et al. Reconditioning of lungs donated after circulatory death with normothermic ex vivo lung perfusion. J Heart Lung Transplant. 2012; 31:187. [PubMed: 22305381]

14. Yeung JC, Cypel M, Waddell TK, van Raemdonck D, Keshavjee S. Update on donor assessment, resuscitation, and acceptance criteria, including novel techniques--non-heart-beating donor lung retrieval and ex vivo donor lung perfusion. Thorac Surg Clin. 2009; 19:261. [PubMed: 19662970]
15. Gazoni LM, Laubach VE, Mulloy DP, et al. Additive protection against lung ischemia-reperfusion injury by adenosine A2A receptor activation before procurement and during reperfusion. J Thorac Cardiovasc Surg. 2008; 135:156. [PubMed: 18179933]
16. LaPar DJ, Laubach VE, Emaminia A, et al. Pretreatment strategy with adenosine A2A receptor agonist attenuates reperfusion injury in a preclinical porcine lung transplantation model. J Thorac Cardiovasc Surg. 2011; 142:887. [PubMed: 21762933]
17. Ross SD, Tribble CG, Linden J, et al. Selective adenosine-A2A activation reduces lung reperfusion injury following transplantation. J Heart Lung Transplant. 1999; 18:994. [PubMed: 10561110]
18. Sharma AK, LaPar DJ, Zhao Y, et al. Natural killer T cell-derived IL-17 mediates lung ischemia-reperfusion injury. Am J Respir Crit Care Med. 2011; 183:1539. [PubMed: 21317314]
19. Sharma AK, Linden J, Kron IL, Laubach VE. Protection from pulmonary ischemia-reperfusion injury by adenosine A2A receptor activation. Respir Res. 2009; 10:58. [PubMed: 19558673]
20. Zhao M, Fernandez LG, Doctor A, et al. Alveolar macrophage activation is a key initiation signal for acute lung ischemia-reperfusion injury. Am J Physiol Lung Cell Mol Physiol. 2006; 291:L1018. [PubMed: 16861385]
21. Yang Z, Sharma AK, Linden J, Kron IL, Laubach VE. CD4+ T lymphocytes mediate acute pulmonary ischemia-reperfusion injury. J Thorac Cardiovasc Surg. 2009; 137:695. [PubMed: 19258091]
22. Gehrau RC, Archer KJ, Mas VR, Maluf DG. Molecular profiles of HCV cirrhotic tissues derived in a panel of markers with clinical utility for hepatocellular carcinoma surveillance. PLoS One. 2012; 7:e40275. [PubMed: 22792259]
23. Mas VR, Maluf DG, Stravitz R, et al. Hepatocellular carcinoma in HCV-infected patients awaiting liver transplantation: genes involved in tumor progression. Liver Transpl. 2004; 10:607. [PubMed: 15108252]
24. Barash Y, Dehan E, Krupsky M, et al. Comparative analysis of algorithms for signal quantitation from oligonucleotide microarrays. Bioinformatics. 2004; 20:839. [PubMed: 14751998]
25. Irizarry RA, Hobbs B, Collin F, et al. Exploration, normalization, and summaries of high density oligonucleotide array probe level data. Biostatistics. 2003; 4:249. [PubMed: 12925520]
26. R Development Core Team. R: A language and environment for statistical computing. Vienna, Austria: R Foundation for Statistical Computing; 2008. http://www.R-project.org
27. Benjamini Y, Hochberg Y. Controlling the false discovery rate: A practical and powerful approach to multiple testing. J R Stat Soc Series B Stat Methodol. 1995; 57:289.
28. Efron B, Tibshirani R. Empirical bayes methods and false discovery rates for microarrays. Genet Epidemiol. 2002; 23:70. [PubMed: 12112249]
29. Reiner A, Yekutieli D, Benjamini Y. Identifying differentially expressed genes using false discovery rate controlling procedures. Bioinformatics. 2003; 19:368. [PubMed: 12584122]
30. Wallinder A, Ricksten SE, Hansson C, et al. Transplantation of initially rejected donor lungs after ex vivo lung perfusion. J Thorac Cardiovasc Surg. 2012; 144:1222. [PubMed: 22995721]
31. Medeiros IL, Pego-Fernandes PM, Mariani AW, et al. Histologic and functional evaluation of lungs reconditioned by ex vivo lung perfusion. J Heart Lung Transplant. 2012; 31:305. [PubMed: 22133788]
32. Pierre L, Lindstedt S, Hlebowicz J, Ingemansson R. Is it possible to further improve the function of pulmonary grafts by extending the duration of lung reconditioning using ex vivo lung perfusion? Perfusion. 2013; 28:322. [PubMed: 23436723]
33. George TJ, Arnaoutakis GJ, Beaty CA, et al. A physiologic and biochemical profile of clinically rejected lungs on a normothermic ex vivo lung perfusion platform. J Surg Res. 2013; 183:75. [PubMed: 23218735]
34. Yeung JC, Wagnetz D, Cypel M, et al. Ex vivo adenoviral vector gene delivery results in decreased vector-associated inflammation pre- and post-lung transplantation in the pig. Mol Ther. 2012; 20:1204. [PubMed: 22453765]

35. Emaminia A, Lapar DJ, Zhao Y, et al. Adenosine A(2) A agonist improves lung function during ex vivo lung perfusion. Ann Thorac Surg. 2011; 92:1840. [PubMed: 22051279]
36. Kreisel D, Goldstein DR. Innate immunity and organ transplantation: focus on lung transplantation. Transpl Int. 2013; 26:2. [PubMed: 22909350]
37. Okusa MD, Linden J, Huang L, Rieger JM, Macdonald TL, Huynh LP. A(2A) adenosine receptor-mediated inhibition of renal injury and neutrophil adhesion. Am J Physiol Renal Physiol. 2000; 279:F809. [PubMed: 11053040]
38. Save S, Mohlin C, Vumma R, Persson K. Activation of adenosine A2A receptors inhibits neutrophil transuroepithelial migration. Infect Immun. 2011; 79:3431. [PubMed: 21646447]
39. Yeung JC, Cypel M, Machuca TN, et al. Physiologic assessment of the ex vivo donor lung for transplantation. J Heart Lung Transplant. 2012; 31:1120. [PubMed: 22975103]
40. Yaar R, Jones MR, Chen JF, Ravid K. Animal models for the study of adenosine receptor function. J Cell Physiol. 2005; 202:9. [PubMed: 15389588]

Abbreviations

$A_{2A}R$	adenosine 2A receptor
EVLP	ex vivo lung perfusion
CSP	cold static preservation
IR	ischemia-reperfusion
DCD	donation after circulatory death
PGD	primary graft dysfunction

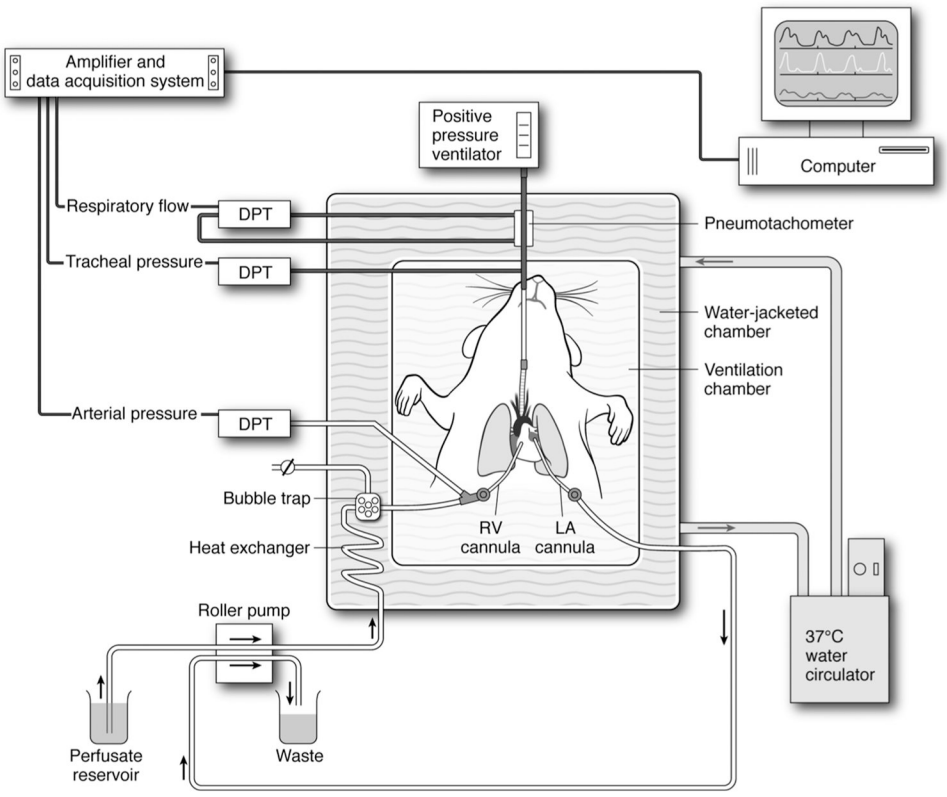

Figure 1. Diagram of the murine EVLP system

An isolated, buffer-perfused mouse lung system (Hugo Sachs Elektronik, March-Huggstetten, Germany) was utilized. The right ventricular (RV) cannula is passed through the pulmonary valve into the pulmonary artery. A left atrial (LA) cannula drains perfusate into waste container. Lungs are perfused at a constant flow of 60 μl/g body wt/min. Lungs are ventilated with room air at 100 breaths/min at a tidal volume of 7 μl/g body weight with a positive end expiratory pressure of 2 cm H_2O using a positive pressure ventilator. The perfusate and lungs are maintained at 37°C by use of a circulating water bath as shown. Air bubbles are removed from the perfusate via a bubble trap as shown. Several differential pressure transducers (DPT) and a pneumotachometer are used to measure arterial pressure, tracheal pressure and respiratory flow via the PULMODYN data acquisition system (Hugo Sachs Elektronik).

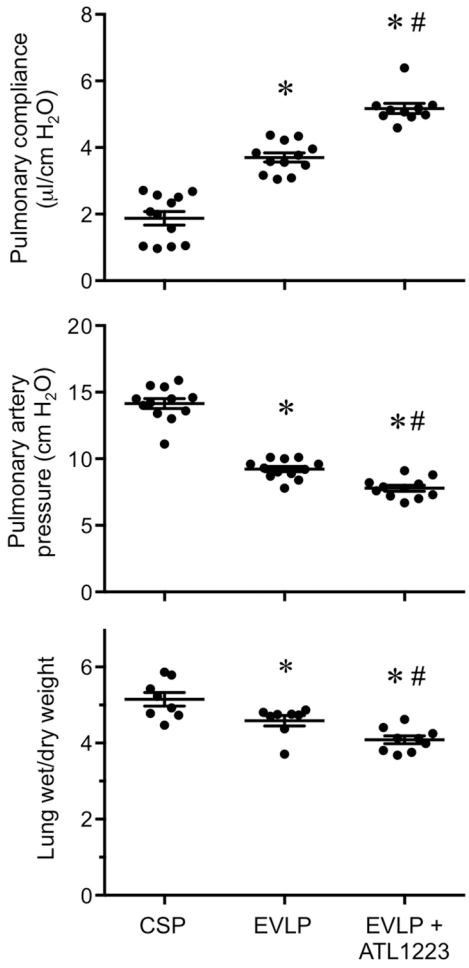

Figure 2. EVLP-directed delivery of ATL1223 improves function and reduces edema in DCD lungs

Compared to lungs after cold static preservation (CSP), EVLP significantly increased pulmonary compliance and reduced pulmonary artery pressure and wet/dry weight (edema). ATL1223 treatment during EVLP provided further, significantly improved lung function and reduced edema. One-way ANOVA with post-hoc Tukey's multiple comparison test was performed to compare groups. Results are presented as mean ± SEM. *p<0.05 versus CSP; $^{\#}p$<0.05 versus EVLP; n=10-12/group (pulmonary compliance and pulmonary artery pressure); n=8-9/group (wet/dry weight).

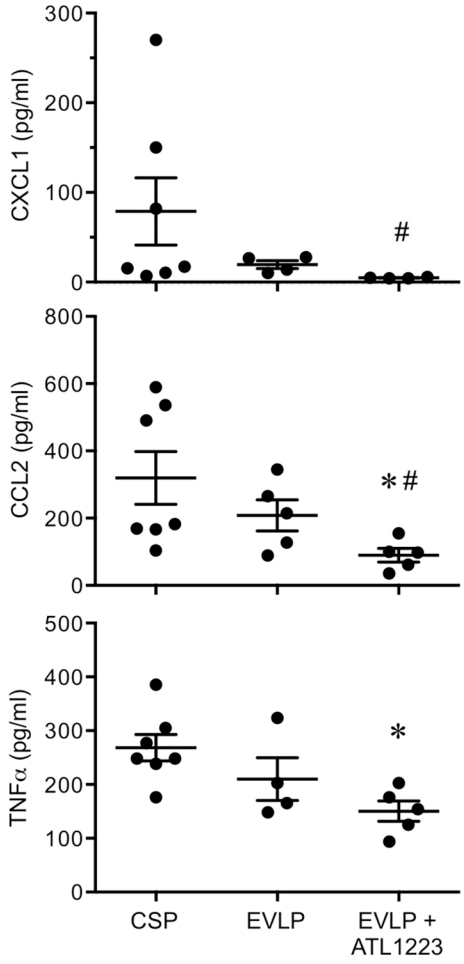

Figure 3. EVLP-directed delivery of ATL1223 reduces proinflammatory cytokine production in DCD lungs

Compared to lungs after cold static preservation (CSP), expression of CXCL1, CCL2 and TNF-α were slightly, but not significantly, reduced by EVLP. ATL1223 treatment during EVLP resulted in significant reductions in expression of CXCL1, CCL2 and TNFα. One-way ANOVA with post-hoc Tukey's multiple comparison test was performed to compare groups. Results are presented as mean ± SEM. *p<0.05 versus CSP; $^{\#}p$<0.05 versus EVLP; n=4-7/group.

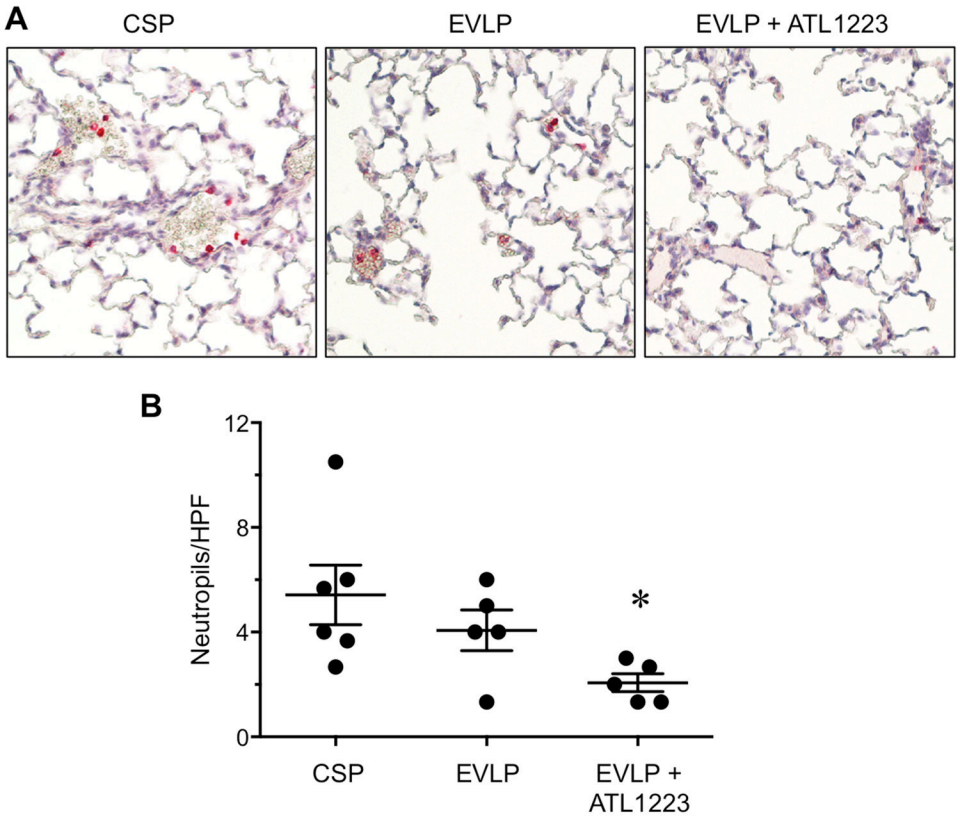

Figure 4. EVLP-directed delivery of ATL1223 depletes pulmonary neutrophils

(A) Representative lung sections (20× magnification) showing immunostaining for neutrophils (red staining). **(B)** Quantitation of the number of neutrophils per high-powered field (HPF) in immunostained lung sections. EVLP with ATL1223 resulted in significantly fewer neutrophils/HPF versus cold static preservation (CSP) and EVLP alone. One-way ANOVA with post-hoc Tukey's multiple comparison test was performed to compare groups. Results are presented as mean ± SEM. *p<0.05 versus all; n=5-6/group.

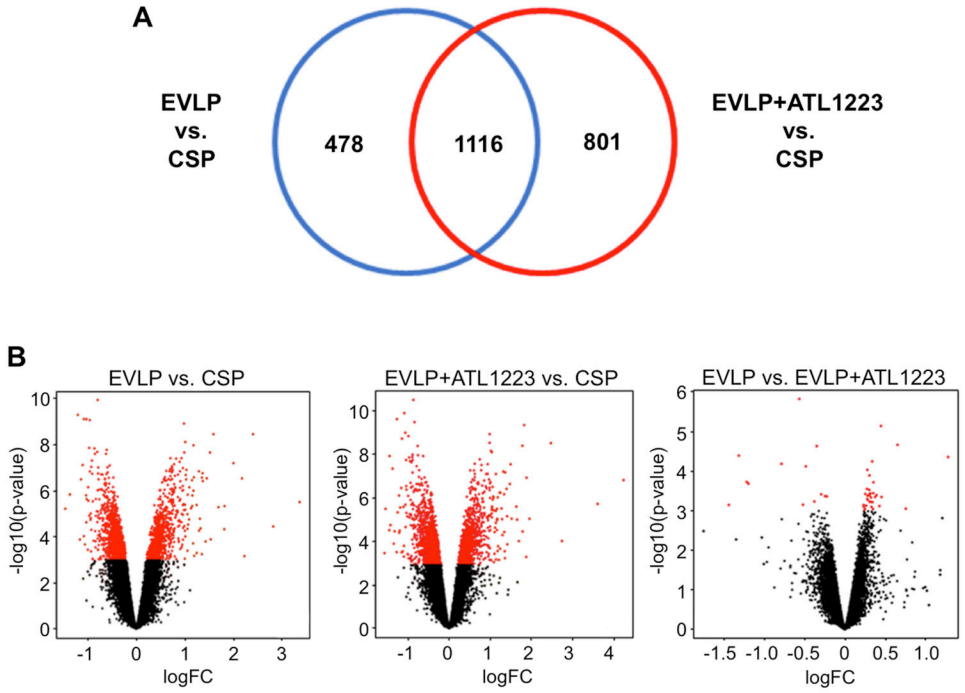

Figure 5. Differentially expressed genes among study groups as a function of EVLP-mediated rehabilitation strategy for DCD lungs

(A) Venn diagram showing numbers of differentially expressed genes in lungs from EVLP and EVLP+ATL1223 groups when compared to the cold static preservation (CSP) control group (FDR 1%). **(B)** Volcano plots depicting the gene expression profile of pairwise comparisons of indicated groups. Each dot represents a unique, differentially expressed probeset. Significant probesets [p-value ≤ 0.001 or –log10 (p-value) ≥ 3] are illustrated by red dots.

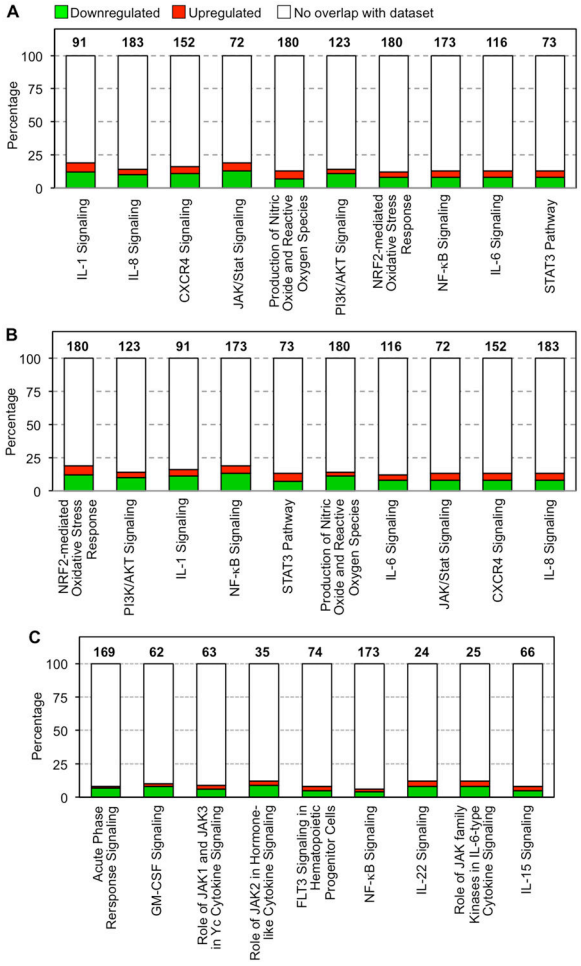

Figure 6. Differentially-expressed canonical pathways affected by EVLP

(A) Ten canonical pathways focused on inflammatory and innate immune responses (selected from the significant canonical pathways in SDC Table 1, $p<0.05$) are shown along the x-axis that are significantly different between EVLP versus CSP. **(B)** Ten canonical pathways focused on inflammatory and innate immune responses (selected from the significant canonical pathways in SDC Table 2, $p<0.05$) are shown along the x-axis that are significantly different between EVLP+ATL223 versus CSP. **(C)** The canonical pathways resulting from the evaluation of genes uniquely differentially expressed in EVLP+ALT1223 vs. CSP (801 genes, FDR 1%). The total number of genes associated with each pathway is listed above each bar. Green and red bars indicate the percentage (y axis) of those genes down- or up-regulated, respectively, as calculated by (# genes in a given pathway that meet cutoff criteria)/(total # genes that comprise that pathway). Pathways are presented left-to-right from highest to lowest significance (specific p values are provided in SDC Tables 1 and 2).

Table 1

Comparison analysis for IL-1 signaling pathway genes between EVLP vs. CSP and EVLP+ATL1223 vs. CSP.

Gene Symbol	Entrez Gene Name	Affymetrix identifier		Gene expression value	
		EVLP vs. CSP (probeset)	EVLP+ATL vs. CSP (probeset)	EVLP vs. CSP (fold change)	EVLP+ATL vs. CSP (fold change)
ADCY9	adenylate cyclase 9	--	1418586_at		-1.3
ECSIT	ECSIT signaling integrator	--	1417080_a_at		-1.2
FOS	FBJ murine osteosarcoma viral oncogene homolog	1423100_at	1423100_at	2.7	2.8
GNA13	guanine nucleotide binding protein (G protein), alpha 13	1422556_at	1422556_at	-1.6	-1.8
GNAI1	guanine nucleotide binding protein (G protein), alpha inhibiting activity polypeptide 1	1427510_at	1427510_at	-1.5	-1.5
GNAI2	guanine nucleotide binding protein (G protein), alpha inhibiting activity polypeptide 2	1435652_a_at	1435652_a_at	1.2	1.2
GNAI3	guanine nucleotide binding protein (G protein), alpha inhibiting activity polypeptide 3	1437225_x_at	1437225_x_at	1.7	1.9
GNAQ	guanine nucleotide binding protein (G protein), q polypeptide	1450115_at	1450115_at	-1.3	-1.2
GNB3	guanine nucleotide binding protein (G protein), beta polypeptide 3	1449159_at	1449159_at	1.3	1.3
GNB4	guanine nucleotide binding protein (G protein), beta polypeptide 4	1419469_at	1419469_at	-1.4	-1.4
IRAK1	interleukin-1 receptor-associated kinase 1	--	1460649_at		-1.2
JUN	jun proto-oncogene	1417409_at	1417409_at	2.0	2.2
MAPK12	mitogen-activated protein kinase 12	--	1449283_a_at		-1.4
MAPK14	mitogen-activated protein kinase 14	--	1426104_at		1.5
PRKAG1	protein kinase, AMP-activated, gamma 1 non-catalytic subunit	1433533_x_at	1433533_x_at	1.7	1.5
TOLLIP	toll interacting protein	--	1423047_at		-1.2
TRAF6	TNF receptor-associated factor 6, E3 ubiquitin protein ligase	1435350_at	1435350_at	-1.3	-1.3

A descriptive list of genes associated with the IL-1 signaling canonical pathway between group comparisons is shown. The number of genes down-regulated (negative fold change) in the EVLP+ALT1223 (EVLP+ATL) *vs*. CSP (cold static preservation) comparison is higher than the EVLP *vs*. CSP comparison.